Ocean Systems Engineering, *Vol. 6, No. 3 (2016) 217-231*
DOI: http://dx.doi.org/10.12989/ose.2016.6.3.217

An adaptive method of multi-scale edge detection for underwater image

Liu Bo*

Dalian Scientific Test and Control Technology Research Institute, 116013 Dalian, Liaoning, China

(Received June 1, 2016, Revised August 12, 2016, Accepted August 30, 2016)

Abstract. This paper presents a new approach for underwater image analysis using the bi-dimensional empirical mode decomposition (BEMD) technique and the phase congruency information. The BEMD algorithm, fully unsupervised, it is mainly applied to texture extraction and image filtering, which are widely recognized as a difficult and challenging machine vision problem. The phase information is the very stability feature of image. Recent developments in analysis methods on the phase congruency information have received large attention by the image researchers. In this paper, the proposed method is called the EP model that inherits the advantages of the first two algorithms, so this model is suitable for processing underwater image. Moreover, the receiver operating characteristic (ROC) curve is presented in this paper to solve the problem that the threshold is greatly affected by personal experience when underwater image edge detection is performed using the EP model. The EP images are computed using combinations of the Canny detector parameters, and the binaryzation image results are generated accordingly. The ideal EP edge feature extractive maps are estimated using correspondence threshold which is optimized by ROC analysis. The experimental results show that the proposed algorithm is able to avoid the operation error caused by manual setting of the detection threshold, and to adaptively set the image feature detection threshold. The proposed method has been proved to be accuracy and effectiveness by the underwater image processing examples.

Keywords: underwater image; bi-dimensional empirical mode decomposition; edge detection; multiple pixel edge features; phase congruency

1. Introduction

Underwater image edge detection is one of the key technologies in underwater image processing technique, which has been widely used in some areas such as ocean surveillance, seabed prospect and underwater targets detection. Consequently, underwater image processing method plays an important role in modern ocean engineering. In general, underwater image with high resolution may be obtained by an underwater camera. In deep-sea or turbid water, however, there will be various image distresses due to the bad illumination conditions and the noisy imaging environments, the image distresses will affect the application of underwater image in underwater targets detection. In order to solve the problem of the various image distresses, scientists have long sought numerous underwater imaging designs, and believing that they can overcome these difficulties (Jaffe 1998, 2001, Nevis 1999). For reducing the effects of sun light scattering and

*Corresponding author, Dr., E-mail: liubo_1977@126.com

http://www.techno-press.org/?journal=ose&subpage=7 ISSN: 2093-6702 (Print), 2093-677X (Online)

absorption on underwater image, especially in turbid water, underwater acoustic imaging (Boyle 2003, Blair 2006) and underwater laser imaging (Nevis 1999, Chen 2002, Chen and Wu 2004) have experienced a spectacular increase in underwater application over recent years. Among these imaging approaches, the mildest drawback is these methods depending on the imaging systems. For the most of underwater images, the underwater optical image will be inevitably encountered. Therefore, this paper will propose a novel method of multi-scale edge detection for underwater optical image analysis, and the algorithm is developed based on the phase-based edge detection utilizing the bi-dimensional empirical mode decomposition (BEMD) technique.

The BEMD method is a two-dimensional extension of the concept of one-dimensional empirical mode decomposition (EMD). The EMD (Huang *et al.* 1998) algorithm is first proposed by Huang, Shen, Long and Wu *et al.* for analyzing non-linear and non-stationary data. This method is initially limited to real-valued time series, and then it has been extended to complex-valued time series (Rilling *et al.* 2007), and has been extended from one dimension to two dimensions, this two-dimensional data decomposition method has been received large attention by the researchers of image analysis (Bhuiyan *et al.* 2008, Damerval *et al.* 2005, Nunes *et al.* 2003 and 2005, Nunes *et al.* 2003, Xu *et al.* 2006). Therefore, this promising image processing technique can be applied in various real problems, for example, image texture analysis (Nunes *et al.* 2003, 2005, Nunes *et al.* 2003, Xu *et al.* 2006), image feature detection (Bhuiyan *et al.* 2008, Ge *et al.* 2007), image denoising (Bhuiyan and Adhami *et al.* 2008), pattern analysis, multi-spectral image fusion (Xu *et al.* 2007) and so on.

The purpose of underwater optical image analysis is to distinguish objects in water and to catch more underwater environment information. The traditional image processing method will lose plenty of features information, but the BEMD approach is to detect more edge information by decomposing multi-layer underwater image. The edge thinning is performed by the Canny operator, and this process also requires manual choice of the threshold parameter. Manual procedure is time-consuming, so aiming at this problem this paper presents a novel feature detection algorithm based on the ROC theory to extract the multi-scale edges of image.

For convenience of discussion, this paper is organized as follows: First, the proposed EP model is represented in section 2 of this paper. Section 3 briefly introduces image edges detection based on ROC curve analysis. In Section 4, two groups of experiments are performed to verify the effectiveness of the proposed algorithm: one is decomposing the test image into IMFs and residues by the BEMD algorithm, the other is detecting the edge information in the first three EPs by the Canny operator and ROC curve analysis. Finally, Section 5 gives concluding remarks.

2. The EP edge detection model for underwater image

Image features such as step edges, lines, and the Mach bands all give rise to point where the Fourier components of an image are maximally in phase. The use of phase congruency for marking image features has significant advantages over the gradient-based method, since the phase congruency is an illumination and contrast invariant measure of the image feature, unlike the gradient-based feature detectors, which can only detect step features. Consequently, this paper provides an edge detection method for underwater image, which is the method of the combination of BEMD algorithm and phase information. For purposes of discussion, this edge detection algorithm is called “EP” model (E denotes the EMD algorithm, P denotes the phase information). As an image edge features extraction tool, the phase-based edge detection (Kovesi 1999) reflects the behavior of an image in the frequency domain, and it has been noted that edge features have many of their frequency components in the same phase. But this method's disadvantages are that calculating the phase congruency map of an image is very computationally intensive, and sensitive to image noise.

In this section, the BEMD algorithm and phase information under which the EP model is designed for the underwater image multi-scale edge detection. Firstly, a 2-D image function $f(x, y)$ can be decomposed into several IMFs sub-images and residual sub-images by the BEMD method, which making the image possible to be shown in multiple scales. Secondly, the multiple-scale edge detection model of an image will be designed based on the multiple-scale image. For each IMF sub-image, the EP model is shown as follows

$$\mathrm{EP} = \mathrm{PC}(\mathrm{IMF}) \tag{1}$$

According to the above analysis, this section gives a specific the description of the multi-scale edge detection process:

(1) The 2-D image function $f(x, y)$ is decomposed by the BEMD algorithm

In order to identify all the local extreme points of the given image $f(x, y)$, there are many methods available for them, such as morphological operators (Nunes 2003, 2005), and sliding window (Bhuiyan *et al.* 2008). These extreme points data interpolation is usually performed by the Delaunay triangulation, the bi-cubic spline, finite element algorithm and two order statistics filters estimation (Bhuiyan *et al.* 2008). In this paper, the regional-based operators will be chose to find the local maxima and minima points from the underwater image data. The regional-based operator assumes that one pixel of image is considered as a local extreme point, if it's value is lower or higher than all of it's neighbors, through scanning each pixel of all image line by line. The surfaces interpolation is realized using the RBF. Moreover, the envelop surface of maximum $E_{\max}(x, y)$ and the envelop surface of minimum $E_{\min}(x, y)$ will be acquired, and then the mean of these envelop surface will be also computed. If $E_{mean}(x, y)$ denotes the average value of envelop surface of extremes, then the formula of it is shown as the following (Liu and Lin 2012)

$$E_{mean}(x, y) = \frac{E_{\max}(x, y) + E_{\min}(x, y)}{2} \tag{2}$$

The difference between the original image's function $f(x, y)$ and $E_{mean}(x, y)$ is the first component, which is designated as $H_1(x, y)$, that is

$$H_1(x, y) = f(x, y) - E_{mean}(x, y) \tag{3}$$

Since the sifting process serves two purposes, viz. to eliminate riding waves and to make the wave-profiles more symmetric. So the procedure should be repeated k times, until H_{1k} is an IMF, that is

$$H_{1(k-1)}(x, y) - E_{mean,k}(x, y) = H_{1k}(x, y) \tag{4}$$

Set $C_1(x, y) = H_{1k}(x, y)$, then $C_1(x, y)$ is the first IMF component separated from the original image data. Similar to the EMD algorithm, a criterion must be determined for each layer of the sifting process to stop, which can be accomplished by limiting the size of the standard deviation

(SD), computed from the two consecutive sifting results $H_{i(k-1)}(x,y)$ and $H_{ik}(x,y)$ for the i *th* mode as (Bhuiyan *et al.* 2008)

$$SD=\sum_{x=1}^{X}\sum_{y=1}^{Y}\left(\frac{\left|H_{i(k-1)}(x,y)-H_{ik}(x,y)\right|^2}{H_{i(k-1)}^2(x,y)}\right) \tag{5}$$

generally, the value of SD is equal or greater than 0.2 meanwhile equal or lesser than 0.3.

After that, $C_1(x,y)$ is separated from the original image data, the rest part is the residue $R_1(x,y)$, it will be treated as the new data and subjected to the same sifting process as described similar to the EMD method, this procedure can be repeated n times, finally the superposition expression will be obtained as follows

$$f(x,y)=\sum_{n=1}^{N}c_n(x,y)+r_n(x,y) \tag{6}$$

where $f(x,y)$ denotes the original image function, $c_n(x,y)$ is designated the information of the smaller scale after the decomposition, $r_n(x,y)$ denotes the final coarsest scale mean trend.

(2) The multiple-scale sub-image edge detection process analysis

For every $c_n(x,y)$, set

$$\mathrm{IMF}_n(x,y)=c_n(x,y),\ (n=1,2,\cdots,N) \tag{7}$$

For every sub-image $\mathrm{IMF}_n(x,y)$, the local energy of the sub-image $E_n(x,y)$ is calculated by the Log-Gabor Wavelet, and the sum of its amplitude $\sum_u|Fp_u|$ is also computed. The minimal scale filter responds to the image noise which is estimated in all directions from the energy figure, the total energy of noise T_n can be obtained in all directions.

The phase congruency of each sub-image is calculated by the following equation (Kovesi 1999)

$$\mathrm{PC}(x,y)=\frac{\lfloor E_n(x,y)-T_n\rfloor}{\sum_u|Fp_u|+\varepsilon} \tag{8}$$

where $\lfloor\bullet\rfloor$ denotes that the difference between the functions is not permitted to become negative, an ε value of 0.01 has been used for all the results presented in the text.

Having defined EP model, from the Eqs. (1), (7) and (8), the n levels multiple-scale sub-image is defined as

$$\mathrm{EP_n}\ =\ \mathrm{PC}(\mathrm{IMF_n}) \tag{9}$$

In this paper, Emphasis is placed on the construction of the EP model by the underwater image analysis in achieving the multiple-scale edges of objectives becomes possible, thus the effect of edge detection in water will rise sharply.

3. The EP edge detection model based on ROC curve analysis

In this paper, the test image is decomposed into IMFs and residues by the EP model. As the first three IMFs (IMF1, IMF2 and IMF3) closely resemble the edge map of an image, so the edges detection is performed in IMFs images by Canny operator. The Canny algorithm detects edges by looking for local maxima of the gradient of image. The gradient's amplitude and orientation are calculated using the derivative of a Gaussian filter. The Canny operator belongs to primarily gradient-based method. But one major issue with the Canny algorithm is it's threshold parameter not automatic caused by the Canny operator, so the ROC (Macmillan *et al.* 1991) curves analysis is employed to select the Canny detector parameter values in this paper.

(1) Generation of underwater image edge extraction

In this step, an image edge extraction graph is automatically constructed, given a range of detection results obtained from different Canny detector parameter sets. The range of parameters to be tested should be large enough to cover a wide range of detection results from noisy to sparse. The actual parameter values depend on the actual implementation setup such as the image intensity range and size. The standard deviation of the Gaussian in the Canny detector here is from 0.9 to 1.5 in steps of 0.2, the high threshold value is from 0.07 to 0.37 in steps of 0.1, and the low threshold is set to one third of the high. Thus, we can implement 16 parameter sets combinations and obtain 16 edge detection graphs. These $N=16$ edge detection results $D_j\,(j=1,2,\cdots,N)$ are then tested for correspondence. A pixel location identified as an edge by all *N* detector setups will have the highest correspondence, and a location identified as an edge by only one detector setup will have the lowest. Typically, points with higher correspondence belong to more distinct luminance edges and are considered to be more related to boundaries of main objects in the image rather than noise or minor features that may appear disturbing to the viewer (Yitzhaky *et al.* 2003). In this paper, *N* detection results will produce *N* possible correspondence levels, so *N* possible correspondence threshold (*CT*) values can be applied to distinguish between points with correspondence higher, equal or lower than that *CT*.

(2) Construction of a ROC curve

To form the *CT*-ROC curve, the *CT* value is applied at each of the *N* correspondence levels. In each *CT* level i, points with correspondence above or equal to the *CT* will be considered as edges and the other points will be considered as non-edges, so a potential ground truth (PGT_i) is formed for each *CT* level i. For each PGT_i $(i=1,2,\cdots,N)$ and each $D_j\,(j=1,2,\cdots,N)$, here, set TP_{PGT_i,D_j}, FP_{PGT_i,D_j}, TN_{PGT_i,D_j} and FN_{PGT_i,D_j} are, respectively, the true positive (*TP*), false positive (*FP*), true negative (*TN*) and false negative (*FN*) in goals, according to the ROC theory, the average of these probabilities in goals are as follows

$$\begin{cases}\overline{TP}_{PGT_i}=\frac{1}{N}\sum_{j=1}^{N}TP_{PGT_i,D_j}=\frac{1}{N}\sum_{j=1}^{N}\left(\frac{1}{RC}\sum_{r=1}^{R}\sum_{c=1}^{C}PGT_{i1}\cap D_{j1}\right)\\ \overline{FP}_{PGT_i}=\frac{1}{N}\sum_{j=1}^{N}FP_{PGT_i,D_j}=\frac{1}{N}\sum_{j=1}^{N}\left(\frac{1}{RC}\sum_{r=1}^{R}\sum_{c=1}^{C}PGT_{i1}\cap D_{j0}\right)\\ \overline{TN}_{PGT_i}=\frac{1}{N}\sum_{j=1}^{N}TN_{PGT_i,D_j}=\frac{1}{N}\sum_{j=1}^{N}\left(\frac{1}{RC}\sum_{r=1}^{R}\sum_{c=1}^{C}PGT_{i0}\cap D_{j0}\right)\\ \overline{FN}_{PGT_i}=\frac{1}{N}\sum_{j=1}^{N}FN_{PGT_i,D_j}=\frac{1}{N}\sum_{j=1}^{N}\left(\frac{1}{RC}\sum_{r=1}^{R}\sum_{c=1}^{C}PGT_{i0}\cap D_{j1}\right)\end{cases}\tag{10}$$

where R and C are the dimension number of image, PGT_{i1} and PGT_{i0} are the pixels in the PGT_i decided as the edges and the non-edges, respectively, and D_{j1} and D_{j0} are, respectively, pixels detected as the edges and the non-edges in the detection j.

Then, according to the ROC theory, the average *TP* rate (*TPR*) and the average *FP* rate (*FPR*) are

$$\begin{cases} TPR_{PGT_i} = \dfrac{\overline{TP}_{PGT_i}}{\overline{TP}_{PGT_i} + \overline{FN}_{PGT_i}} \\ FPR_{PGT_i} = \dfrac{\overline{FP}_{PGT_i}}{\overline{FP}_{PGT_i} + \overline{TN}_{PGT_i}} \end{cases} \tag{11}$$

where, $P = \overline{TP}_{PGT_i} + \overline{FN}_{PGT_i}$, $1 - P = \overline{FP}_{PGT_i} + \overline{TN}_{PGT_i}$; the *TPR* and *FPR* are known as sensitivity and (1- specificity), respectively. So the coordinates of these points' pairs (*FPR*, *TPR*) are forming a curve, which is the *CT*-ROC curve.

4. The results and discussion of the preliminary experiment

4.1 Multi-scale decomposition of underwater image based on BEMD algorithm

This section gives a specific example of BEMD algorithm, the original test images shown in Figs. 1 and 2 are as follows

Fig. 1 Img1

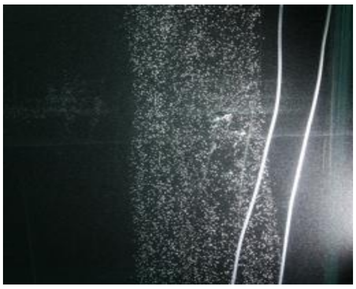

Fig. 2 Img2

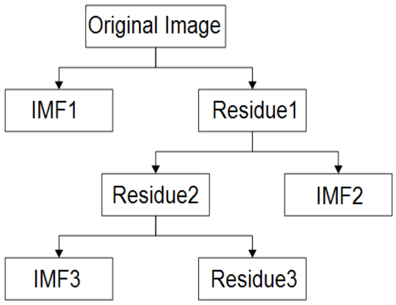

Fig. 3 Decomposition diagram of BEMD

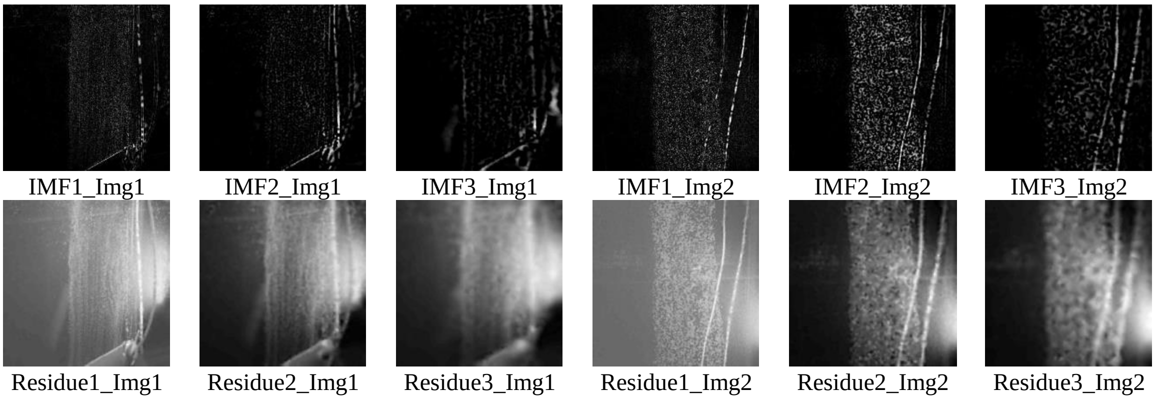

Fig. 4 Test image 1 and test image 2 are decomposed into three IMFs and three Residues

The Fig. 3 displays three layers decomposition of the original image based on BEMD, this procedure can separate natural scale from the original image to achieve image decomposition from low to high frequency. To begin with, the first intrinsic mode function (*IMF1*) is separated from the original image, which corresponds to the image with the highest spatial frequency. The residue (viz. *Residue1*), is the remainder which the *IMF1* is subtracted from the original image, and it corresponds to the image with the lowest spatial frequency. The next step is to extract the *IMF2* in the *Residue1*, and obtains the *Residue2*. In the end, the *IMF3* and *Residue3* can be obtained in the same way. Each IMF is obtained through decomposing the upper residue image, as shown in Fig. 4; the test image is decomposed into three IMF images and three residual images, the first row is IMF image from finer to courser scales, the second row displays the residue image corresponding to the IMF. The IMF image represents the texture, noise and edges information of underwater image. The *IMF1* obviously exhibits edges information of image, and the residue image presents the basic structure and eventual trend of image.

Fig. 5 is the edge detection map by the proposed method. This is a group of gas curtain images under water; though it is impossible to distinguish the sizes and amounts of bubbles in image, the large quantities of texture information about objects are still obtained in the EP images. In general, there are some problems with non-structured objects such as bubbles and rocks in underwater image; it is difficult to extract the robust information from these images. In Figs. 4 and 5, however, a lot of information about these non-structured objects can be acquired by comparing analysis. Moreover, the EP image has good visual effect over the IMF image. The Fig. 5 second row gives the relation between phase angle and frequency in each EP sub-image. It can be seen that the phase angle $\pi/2\,(\approx 1.57)$ is a knee of the curve.

In each EP image, the local energy $E_n(x, y)$ is calculated by the Log-Gabor Wavelet, Table 1 and Table 2 are shown the mean energy squared values recorded with smallest scale filter at each orientation, the mean energy values are reduced along with the increasing number of the EP layers.

As pointed out by Kovesi (Kovesi 2002), the weighted mean phase angle will lie in the range $-\pi$ to $+\pi$. As one moves around the phase circle an angle of zero indicates an upward going step, $\pi/2$ indicates a bright line feature, π indicates a downward going step, and $3\pi/2$ indicates a dark line feature. Our EP model inherits this trait, the weighted mean phase angle 0 and π correspond to a line, and the angle $\pi/2$ and $3\pi/4$ correspond to a step, as shown in the Fig. 6.

Table1 Mean Energy squared values of test image 1

	0	$\pi/4$	$\pi/2$	$3\pi/4$	π	$3\pi/2$
EP1	1.8201	1.0951	0.7524	0.7782	0.7536	1.0793
EP2	0.0770	0.0592	0.0548	0.0574	0.0579	0.0604
EP3	0.0040	0.0029	0.0032	0.0036	0.0031	0.0026

Table 2 Mean Energy squared values of test image 2

	0	$\pi/4$	$\pi/2$	$3\pi/4$	π	$3\pi/2$
EP1	5.1250	3.5791	2.9446	2.8239	2.8239	3.9320
EP2	0.2789	0.2250	0.2040	0.2108	0.2125	0.2449
EP3	0.0082	0.0073	0.0074	0.0077	0.0075	0.0075

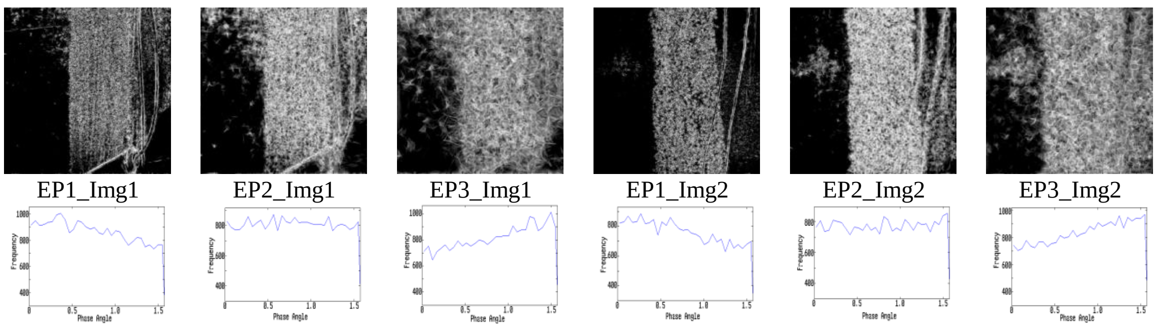

Fig. 5 EP image and its frequency

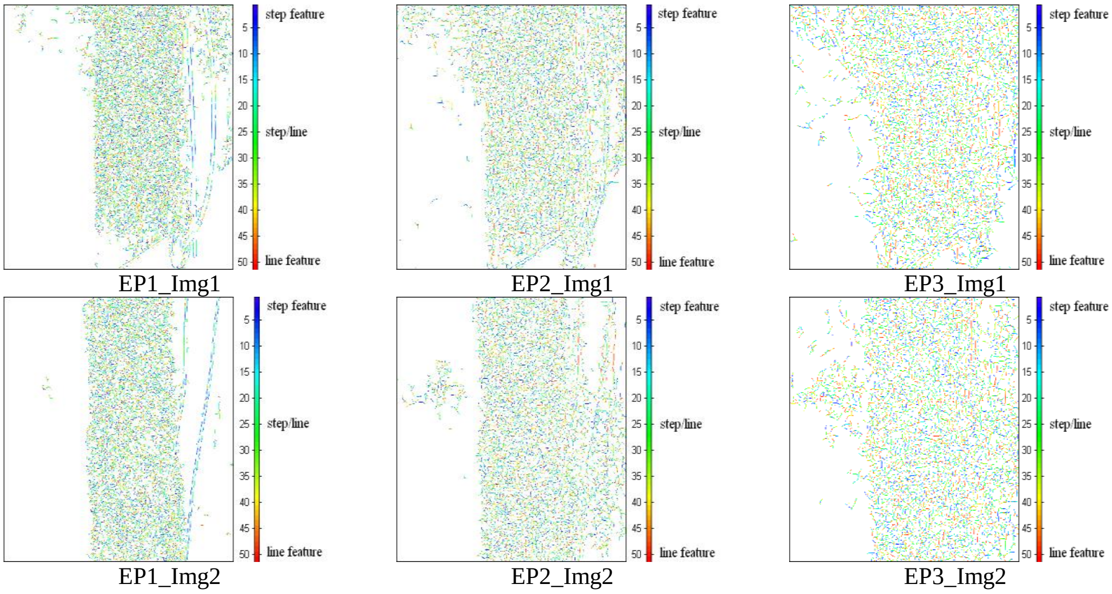

Fig. 6 Edge types analysis

4.2 Results of edge features detection based on CT-ROC curve

A histogram of the correspondence for $N = 16$ is presented in Fig. 7. Examples of the PGT_i s with *CT* level $i = 4$ are presented in Fig. 8.

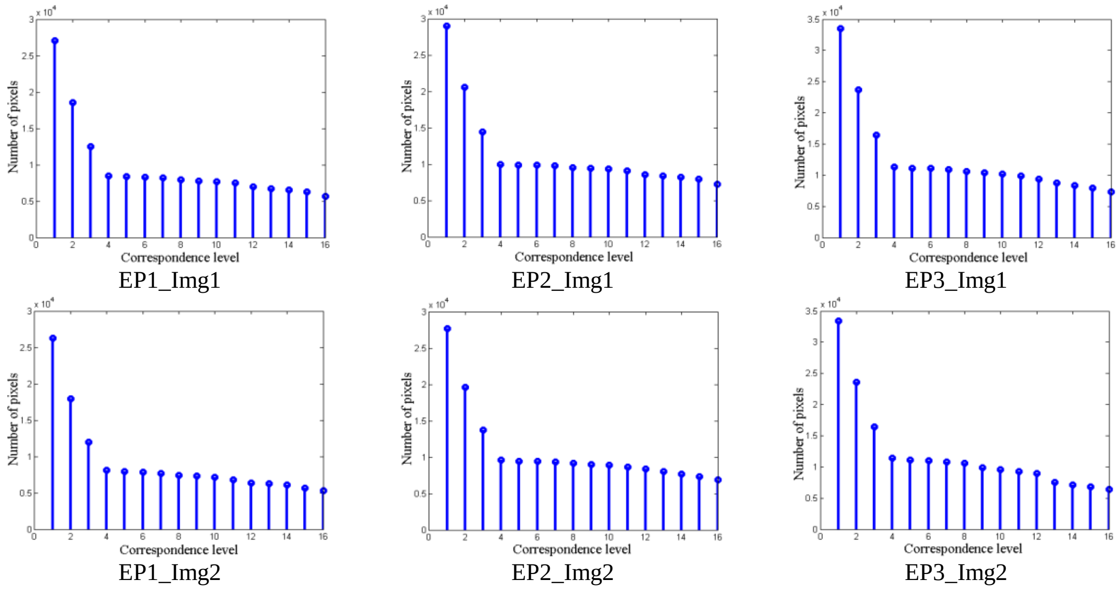

Fig. 7 Correspondence level of every EP image edge pixels

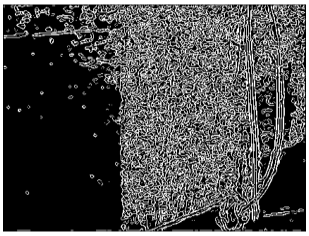

EP1_Img1

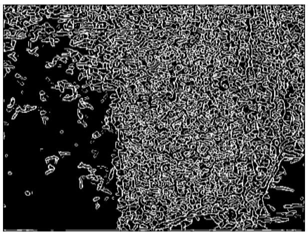

EP2_Img1

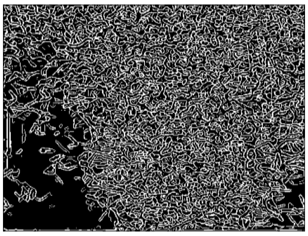

EP3_Img1

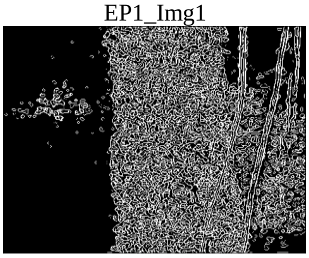

EP1_Img2

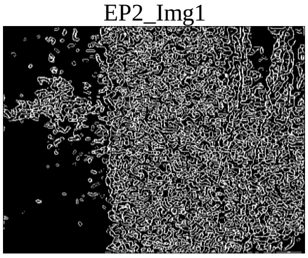

EP2_Img2

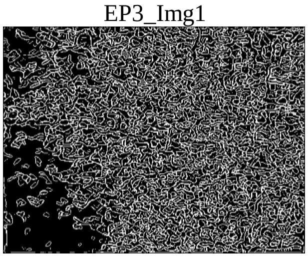

EP3_Img2

Fig. 8 PGT edge map

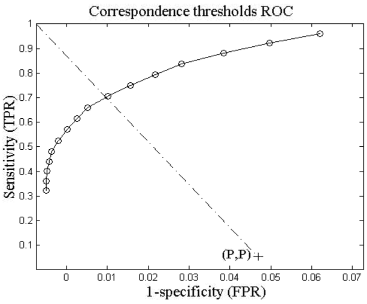

EP1_Img1

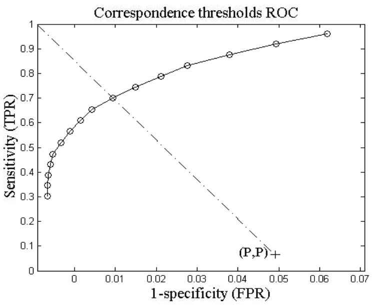

EP2_Img1

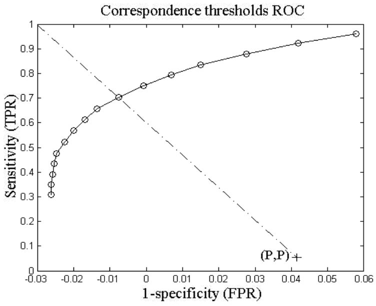

EP3_Img1

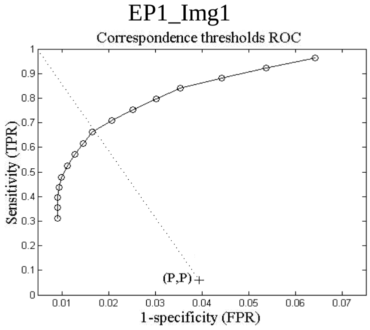

EP1_Img2

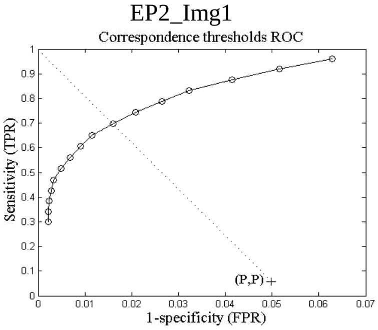

EP2_Img2

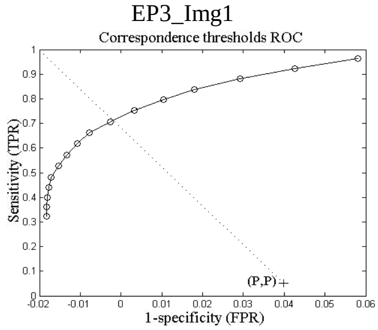

EP3_Img2

Fig. 9 ROC curve of each EP image

ROC analysis is applied here to find the best *CT* value that forms the PGT by considering the trade off between increasing the information and decreasing the noise in the detection result. The best *CT* value is defined as the one that forms a PGT giving the best match to the entire edge detection results. This PGT will be our ideal edge graph. The optimal *CT* forms a point in the *CT*-ROC plane that is the closest to the ideal point (0, 1). As shown in Fig. 9, we define a diagnosis line by connecting the points (P, P) and (0, 1) on the *CT*-ROC plane. Then, the best *CT* value will be at the intersection of the diagnosis line and the ROC curve (Yitzhaky *et al.* 2003), and practically the closest point to the intersection. Thus, the ideal edge graphs are show in Fig. 10.

4.3 Results of edge segmentation using the EP model

This experiment will segment the every EP sub-image using the region growing method (Theo 1990), as illustrated in the Fig. 11, let's only take the first two EP image of Img1 for example. Firstly, the each EP sub-image is extracted edge features by the EP model; the next step will perform the edge segmentation according to the region growing algorithm in every EP sub-image; finally, this paper provides the statistical analysis on the change of the pixel of each EP sub-image.

5. Conclusions

The BEMD algorithm is a potential image processing method, which is not only robust and adaptive, but also totally data-driven. The phase congruency is a measure of feature significance in computer image; this edge detection is particularly robust against changes in illumination and contrast. In this paper, the EP model is the phase congruency multi-scale edge detection based on the BEMD algorithm, which inherits theirs good traits. The contrast experiment has shown that, the proposed method could detect a lot of edge features information for underwater image, even for unclear image. The experiment also provides some satisfactory results of this paper, which are summarized as follows

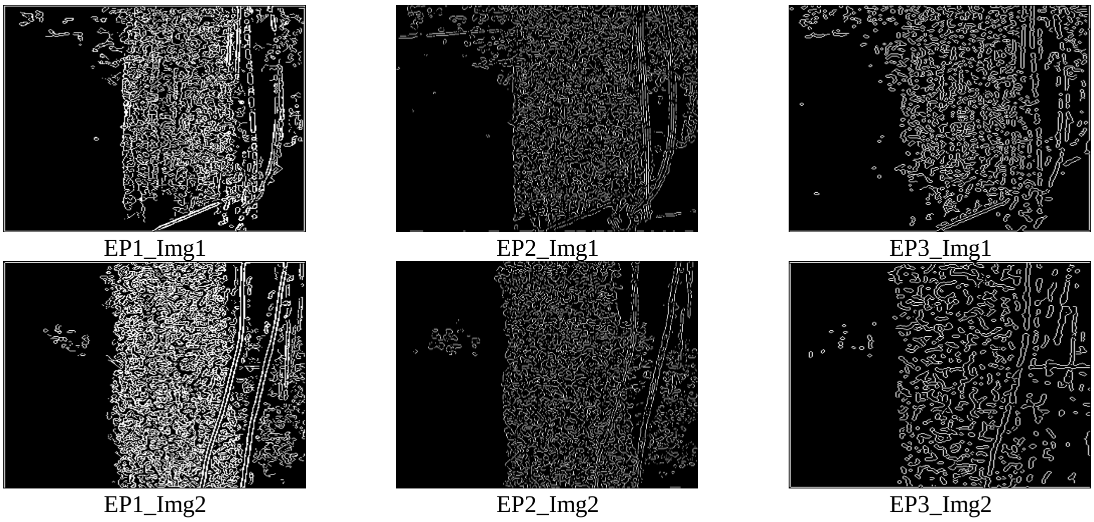

Fig. 10 Ideal edge extraction using the optimal CT value

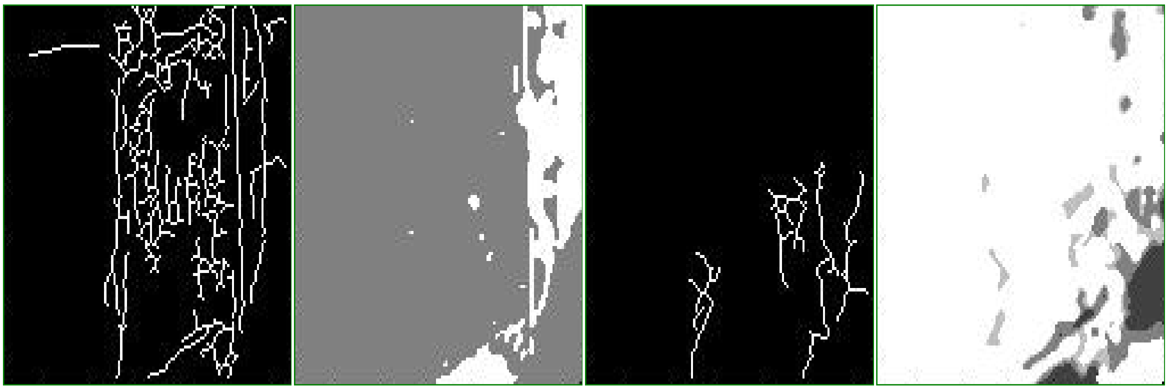

EP1_Img1 edge map EP1_Img1 segmentation EP2_Img1 edge map EP2_Img1 segmentation

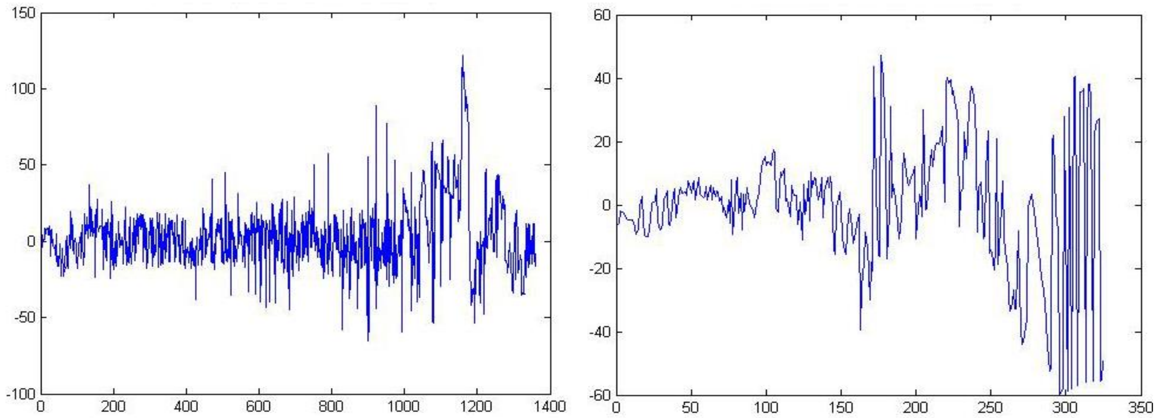

The change of EP1_Img1 edge pixel The change of EP2_Img1 edge pixel

Fig. 11 The region segmentation analysis of underwater image by the EP model

(1) In view of some virtues of the BEMD algorithm and the phase congruency theory, this paper has successfully proposed the EP model to process underwater image. The EP model inherits the advantages of the first two methods accordingly.

(2) The image segmentation is performed based on the principle of the multi-scale edge detection of image. So it is feasible that the underwater image could be segmented by means of multiple scales.

(3) The EP model could make full use of the texture information of every layer sub-image, which is its peculiar trait.

Conclusively, as described by this article, it enables us to realize that the image processing technology has a wide range of applications in underwater engineering, and is obviously of crucial significance.

Acknowledgements

This study is supported by the "Liaoning BaiQianWan" Talents Program (2013-186-25), the Program of Scientific Research Project of Liao Ning Province Education Commission (LS2013046), and the National Commonweal Industry Scientific Research Project (201303024).

References

Bhuiyan, S.M.A, Adhami, R.R., Ranganath, H.S. *et al*. (2008c), "Aurora image denoising with a modified bi-dimensional empirical mode decomposition method", *Proceedings of the IEEE Southeast Con 2008*, Alabama: Institute of Electrical and Electronics Engineers, Huntsville, USA.

Bhuiyan, S.M.A., Adhami, R.R. and Khan, J.F. (2008), "Edge detection via a fast and adaptive bidimensional empirical mode decomposition", *Proceedings of the Machine Learning for Signal Processing*, Cancun, Mexico: IEEE Signal Processing Society.

Bhuiyan, S.M.A., Adhami, R.R. and Khan, J.F. (2008), "Fast and adaptive bidimensional empirical mode decomposition using order-statistics filter based envelope estimation", *J. EURASIP Journal on Advances in Signal Processing*, 2008, 1-18.

Bhuiyan, S.M.A., Adhami, R.R. and Khan, J.F. (2008a), "Fast and adaptive bi-dimensional empirical mode decomposition using order-statistics filter based envelope estimation", *EURASIP J. Adv. Signal Pr.*, 1-18.

Bhuiyan, S.M.A., Adhami, R.R. and Khan, J.F. (2008b), "Edge detection via a fast and adaptive bi-dimensional empirical mode decomposition", *Proceedings of the Machine Learning for Signal Processing*, Cancun, Mexico.

Bhuiyan, S.M.A., Adhami, R.R., Ranganath, H.S. *et al*. (2008), "Aurora image denoising with a modified bidimensional empirical mode decomposition method", *Proceedings of the IEEE Southeast Con 2008*, Huntsville, Alabama: Institute of Electrical and Electronics Engineers.

Blair, D.G. (2006), "Underwater acoustic imaging: image due to a specular reflector in the geometrical-acoustics limit", *J. Marine Sci. Technol*., **11**(2), 123-130.

Blair, D.G. (2006), "Underwater acoustic imaging: image due to a specular reflector in the geometrical acoustics limit", *J. Marine Sci. Technol.*, **11**(2), 123-130.

Boyle, F. (2003), "Image processing techniques for underwater acoustic image enhancement", *J. Acoust. Soc. Am*., **114**(4), 2398-2399.

Boyle, F. (2003), "Image processing techniques for underwater acoustic image enhancement", *J. Acoust. Soc. Am.*, **114**(4), 2398-2399.

Chen, H.H. (2002), "Variation reduction in quality of an optical triangulation system employed for underwater range finding", *J. Ocean Eng*., **29**(15), 1871-1893.

Chen, H.H. (2002), "Variation reduction in quality of an optical triangulation system employed for underwater range finding", *Ocean Eng.*, **29**(15), 1871-1893.

Chen, H.H. and Wu, C.M. (2004), "An algorithm of image processing for underwater range finding by active triangulation", *J. Ocean Eng.*, **31**(8-9), 1037-1062.

Chen, H.H. and Wu, C.M. (2004), "An algorithm of image processing for underwater range finding by active triangulation", *Ocean Eng.*, **31**(8-9), 1037-1062.

Damerval, C., Meignen, S. and Perrier, V. (2005), "A fast algorithm for bidimensional EMD", *J. IEEE Signal Processing Letters*, **12**(10), 701-704.

Damerval, C., Meignen, S. and Perrier, V. (2005), "A fast algorithm for bi-dimensional EMD", *J. IEEE Signal Processing Letters*, **12**(10), 701-704.

Ge, G.T., Sang, E.F., Liu, Z.F. *et al*. (2007), "Underwater acoustic feature extraction based on bi-dimensional empirical mode decomposition in shadow field", *Proceedings of the signal design and its applications in communications*, Southwest Jiaotong University, Chengdu, China.

Guangtao, G.E., Enfang, S., Zhuofu, L. *et al*. (2007), "Underwater acoustic feature extraction based on bidimensional empirical mode decomposition in shadow field", *Proceedings of the signal design and its applications in communications*, Chengdu: Southwest Jiaotong University.

Huang, N.E., Shen, Z., Long, S.R. *et al.* (1998), "The empirical mode decomposition and the Hilbert spectrum for nonlinear and non-stationary time series analysis", *J. Proceedings of the Royal Society of London: Mathematical, Physical and Engineering Sciences*, **454**(1971), 903-995.

Huang, N.E., Shen, Z., Long, S.R. *et al.* (1998), "The empirical mode decomposition and the Hilbert spectrum for nonlinear and non-stationary time series analysis", *Proceedings of the Royal Society of London*: *Mathematical, Physical and Engineering Sciences*, **454**(1971), 903-995.

Jaffe, J.S. (1998), "Underwater optical imaging: the design of optimal systems", *J. Oceanography*, **11**(1), 40-41.

Jaffe, J.S. (1998), "Underwater optical imaging: the design of optimal systems", *Oceanography*, **11**(1), 40-41.

Jaffe, J.S. (2001), "Underwater optical imaging: status and prospects", *J. Oceanography*, **14**(3), 64-75.

Jaffe, J.S. (2001), "Underwater optical imaging: status and prospects", *Oceanography*, **14**(3), 64-75.

Kovesi, P. (1999), "Image features from phase congruency", *J. Videre: J. Comput. Vision Res*., **1**(3), 1-27.

Kovesi, P. (1999), "Image Features from Phase Congruency", *Videre*: *J. Comput. Vision Res.*, **1**(3), 1-27.

Kovesi, P. (2002), "Edges are not just steps", *Proceedings of the 5th Asian Conference on Computer Vision*, Melbourne, Australia.

Kovesi, P. (2002), "Edges are not just steps", *Proceedings of the 5th Asian Conference on Computer Vision*, Melbourne, Australia.

Liu, B. and Lin, Y. (2012), "A method for underwater image analysis using bi-dimensional empirical mode decomposition technique", *Ocean Syst. Eng*., **2**(2), 137-145.

Liu, B. and Lin, Y. (2012), "A method for underwater image analysis using bi-dimensional empirical mode decomposition technique", *Ocean Syst. Eng.*, **2**(2), 137-145.

Macmillan, N.A. and Creelman, C.D. (1991), *Detection Theory: A User's Guide*, Cambridge: Cambridge Univ. Press.

Macmillan, N.A. and Creelman, C.D. (1991), *Detection Theory*: *A User's Guide*, Cambridge Univ. Press, Cambridge, U. K.

Nevis, A. (1999), "Adaptive background equalization and image processing applications for laser line scan data", *J. Proceedings of SPIE*, **3710**(2),1260-1271.

Nevis, A. (1999), "Adaptive background equalization and image processing applications for laser line scan data", *Proceedings of SPIE*, **3710**(2), 1260-1271.

Nunes, J.C. and Bouaoune, Y. and Delechelle, E. *et al.* (2003), "Image analysis by bidimensional empirical mode decomposition", *J. Image Vision Comput*., **21**(12), 1019-1026.

Nunes, J.C., Bouaoune, Y., Delechelle, E. *et al*. (2003), "Image analysis by bi-dimensional empirical mode decomposition", *Image and Vision Computing*, **21**(12), 1019-1026.

Nunes, J.C., Guyot, S. and Delechelle, E. (2005), "Texture analysis based on local analysis of the bidimensional empirical mode decomposition", *J. Machine Vision Appl*., **16**(3), 177-188.

Nunes, J.C., Guyot, S. and Deléchelle, E. (2005), "Texture analysis based on local analysis of the bi-dimensional empirical mode decomposition", *Machine Vision and Appl.*, **16**(3), 177-188.

Nunes, J.C., Niang, O., Bouaoune, Y. *et al.* (2003), "Texture analysis based on the bidimensional empirical mode decomposition with gray-level co-occurrence models", J. *IEEE Machine Vision Appl.*, **2**, 633-635.

Nunes, J.C., Niang, O., Bouaoune, Y. *et al*. (2003), "Texture analysis based on the bi-dimensional empirical mode decomposition with gray-level co-occurrence models", *IEEE Machine Vision and Application*, **2**, 633-635.

Rilling, G., Flandrin, P., Goncalves, P. *et al.* (2007), "Bivariate empirical mode decomposition", *J. IEEE Signal Processing Lett*., **14**(12), 936-939.

Rilling, G., Flandrin, P., Goncalves, P. *et al*. (2007), "Bivariate empirical mode decomposition", *J. IEEE Signal Processing Letters*, **14**(12), 936-939.

Theo, P. (1990), "Integrating region growing and edge detection", *J. IEEE Trans. On Pattern Analysis and Machine Intelligence*, **12**(3), 225-233.

Theo. P. (1990), “Integrating region growing and edge detection”, *IEEE Trans. On Pattern Analysis and Machine Intelligence*, **12**(3), 225-233.

Xu Y., Liu, B., Liu, J. *et al.* (2006), “Two-dimensional empirical mode decomposition by finite elements”, *J. Proceedings of the Royal Society A*, **462**(2074), 3081-3096.

Xu, X., Li, H. and Wang, A.N. (2007), “The application of BEMD to multi-spectral image fusion”, *Proceedings of the Wavelet Analysis and Pattern Recognition (ICWAPR)*, Beijing: University of Science & Technology.

Xu, X., Li, H. and Wang, A.N. (2007), “The application of BEMD to multi-spectral image fusion”, *Proceedings of the Wavelet Analysis and Pattern Recognition* (*ICWAPR*), Beijing University of Science & Technology, Beijing, China.

Xu, Y., Liu, B., Liu, J. *et al*. (2006), “Two-dimensional empirical mode decomposition by finite elements”, *Proceedings of the Royal Society A*, **462**(2074), 3081-3096.

Yitzhaky, Y. and Peli, E. (2003), “A method for objective edge detection evaluation and detector parameter selection”, *J. IEEE Transactions on Image Processing*, **25**(8), 1027-1033.

Yitzhaky, Y. and Peli, E. (2003), “A method for objective edge detection evaluation and detector parameter selection”, *IEEE Transactions on Image Processing*, **25**(8), 1027-1033.

MK